Multi-level screening of computation-ready, experimental metal-organic frameworks for natural gas purification

Zhi Li[1, *], Yue Zhang[1], Bei Liu[2, *] and Guangjin Chen[2]

[1]*Shandong Provincial Key Laboratory of Molecular engineering, QiLu University of Technology (Shandong Academy of Sciences), Jinan 250353, China*

[2] *State Key Laboratory of Heavy Oil Processing, China University of Petroleum, Beijing 102249, China*

[1*] Corresponding authors.

E-mail addresses: liz@qlu.edu.cn (Z. Li), liub@cup.edu.cn (B. Liu)

ABSTRACT

In this work, traditional Monte Carlo simulation and DFT-based structural optimization methods were combined to screen computation-ready experimental MOF database for the application of natural gas purification. Our results show that about half of the good performing CoRE-MOF structures displayed various degrees of deformation (even collapse) after the structure optimization. This phenomenon attributed to the strong attraction of unsaturated metals which attract nearby organic components. For some materials with deformation, unsaturated metals form new bonds with the adjacent organic linkers creating distortions that would be unrealistic in the experimental materials. For the remaining relatively stable materials whose structural characteristics did not change too much, we further studied the adsorption performance of their optimized structures. Finally, 12 good-performing MOF materials with high stability were screened out which could greatly improve the possibility for constructing robust MOFs that could hold open metal sites by experiments.

Keywords: metal-organic framework; molecular simulation; gas separation

1. INTRODUCTION

The development and utilization of clean energy becomes more and more urgent and crucial as the energy crisis and environmental concerns. There is mounting interest in developing improvements in clean-burning alternatives, including natural gas. The concentration of CO_2 in underground methane reservoirs is about 10% at the pressure of 10 bar. Eliminating CO_2 in natural gas improves upon an existing commodity, as the presence of CO_2 would decrease the heat value and corrodes the pipeline. In this case, the technology for gas purification must minimize costs in order to achieve wide-spread industrial adoption.

Plenty of techniques have been proposed to solve the problem of purifying CO_2 from these applications including distillation, amine scrubbing, and sorbent adsorption. Among these methods, pressure swing adsorption (PSA) technology is of particular industrial interest for its outstanding energy efficiency and low operating costs[1]. The primary component of a PSA process is the gas sorbent, which is typically a nanoporous material where a high selectivity and large capacity for the target gas are among its desired properties[2]. Metal-organic frameworks (MOFs), with record-high porosity and surface areas as well as tunable pores, are good candidates for PSA processes. It is, however, yet unclear what the optimal material or design principles are for gas separation. Several studies have proposed easy-to-quantify metrics that can distinguish high-performing and low-performing MOFs implemented in a PSA system[3-9] so that one can provide a generalized ranking of materials in a high-throughput screening study. These metrics take into account several competing properties, such as gas selectivity, overall capacity, adsorption enthalpy and regenerability to provide a single value to rate materials.

The search for high-performance materials has recently been advanced by Chung et al., who developed a computation-ready experimental MOF (CoRE-MOF) database for the purposes of being able to rapidly screen existing MOFs, which there are known routes to

synthesis[10]. This database, consisting of nearly 5000 structures, has been manipulated from experimentally reported data to ensure that each material possesses its highest possible void space. In this way, both free-floating and coordinated solvent molecules bound to metal centers have been removed, based on the assumption that this would mimic the effects of experimental activation procedures. While convenient for the identification of potentially optimal MOFs through computational screening, the assumption that the CoRE materials will maintain structural stability following activation may be severe. Indeed, numerous study demonstrated that performance for CO_2 adsorption is highly sensitive to the pore shape of the material[11-13].

In this work, we computationally screen a subset of 2,932 CoRE-MOFs, where partial atomic charges were obtained from the DDEC method and ground-state DFT calculations. Grand canonical Monte Carlo (GCMC) simulations for natural gas separations are performed using these charges. Metrics of adsorption selectivity (S_{ads}) and capacity (ΔN_{co2}) were respectively used to identify high performing materials. To understand if these materials are structurally stable, several high performing materials were optimized at the density functional theory (DFT) level of theory. While we observed interesting ligand coordination phenomena to open metal-sites in some materials, those that survived greatly improve the possibility for constructing robust MOFs that could hold open metal sites by experiments.

2. METHODS:

2.1 Overview

The whole screening process consists of the following steps:

- *Initial screening:* Classical GCMC simulations were used to investigate the adsorption properties of these 2932 CoRE-MOFs for CO_2/CH_4 separation. The state

point for natural gas purification was set to 298K and 10 bar for adsorption and 1 bar for desorption, maintaining the same molar ratio 10:90 for CO_2:CH_4.

- *Structure optimization:* Periodic DFT method was employed to optimize the top 10% performing CoRE-MOF structures based on the product $S_{ads}\times\Delta N_{co2}(CO_2/CH_4)$.
- *The analysis of materials' stability:* By analyzing the geometry changes caused by structural optimization, the stability of fully activated materials was initially predicted.
- *Adsorption performance of relatively-stable materials:* The performance of these stable refined structures was further studied at the same thermodynamic conditions as above. If the optimized stable structures still show good performance, these materials could be treated as good candidates for experimental synthesis and testing.

2.2 Monte Carlo simulation details

Grand-canonical Monte Carlo (GCMC) simulations were used to investigate the adsorption of CO_2/CH_4 gas mixture in MOFs. During the whole GCMC simulation process, the materials were treated as rigid structures ignoring the skeleton stretching and bending vibration. The simulation cells were expanded to at least 24.0 Å along each dimension and the periodic boundary conditions were applied in all three directions. Lennard-Jones (LJ) and Coulombic potentials were combined to calculate the non-bonded interactions:

$$U_{ij} = 4\varepsilon_{ij}\left(\left(\frac{\sigma_{ij}}{r_{ij}}\right)^{12} - \left(\frac{\sigma_{ij}}{r_{ij}}\right)^{6}\right) + \frac{q_i q_j}{4\pi\varepsilon_0 r_{ij}}$$

where i and j are interacting atoms, and r_{ij} is the distance between atoms i and j, ε_{ij} and σ_{ij} are the LJ well depth and collision diameter, respectively, q_i and q_j are the partial charges of the interacting atoms, and ε_0 is the dielectric constant. CO_2 was regarded as a rigid linear molecule with 0.116 nm C-O bond length. The LJ potential parameters of the O atom (σ_O =

0.305nm and ε_O/κ_B=79.0K) and C atom (σ_C = 0.280 nm and ε_C/κ_B = 27.0 K) in the CO_2 molecule were taken from the TraPPE force field[14]. Partial point charges are $q_O = -0.35e$ and $q_C = 0.70e$. CH_4 was represented by a united-atom model (σ = 0.373 nm and ε/κ_B = 148.0 K)[15]. The force field parameters of frameworks were taken from DREIDING[16], and only from UFF[17] when a parameter can not be found in DREIDING. The atomic partial charges of materials derived from DDEC charges[18]. The cross interaction parameters were derived by the Lorentz-Berthelot mixing rules and all electrostatic interactions were computed using the Ewald summation technique[19]. The LJ potential cutoff radius was chosen as r_c=1.20nm and fugacity values obtained by Peng-Robinson equation of state were taken as inputs to calculate the gas adsorption. The total GCMC simulation consisted of 2000 cycles. The first 1000 cycles are for equilibrium, and then last 1000 cycles are for statistical thermodynamics calculation. All the GCMC simulations were carried out using the RASPA package.

The separation performance of materials was estimated by two vital metricsi.e. adsorption selectivity of CO_2 over CH_4 (S_{ads}) and CO_2 working capacity (ΔN_{CO_2}). Selectivity is defined as the ratio of the loading mole fractions divided by the ratio of the gas phase mole fractions. And the working capacity is defined as the difference in loading of each adsorbent at adsorption and desorption condition[20]. In this work, the adsorption and desorption pressure were set to be 10 bar and 1 bar respectively.

2.3 Structure optimization details

Periodic density functional theory (DFT) based geometry optimization procedure was employed to refine these selected top-performing structures and obtained their reliable structures. All the DFT geometry calculations were implemented in the Quantum Espresso code[21] with a plane wave basis. Projector augmented wave (PAW) pseudopotentials with PBEsol[22] functional were used during the process. PBEsol is a revised Perdew-Burke-

Ernzerhof (PBE) generalized gradient approximation that improves equilibrium properties of densely packed solids and their surfaces and thought to be more suitable for solids. BFGS algorithm was used to do variable-cell optimization, allowing for the relaxation of all atoms and cells without symmetry restrictions. The kinetic energy cutoff (Ry) for wave functions was set to be 80 Ry and the kinetic energy cutoff (Ry) for charge density and potential was set to be 600 Ry.

2.4 Calculation of structural properties

The stability of materials upon desolvation was evaluated by analyzing the structural changes caused by geometry optimization. Six structural parameters were considered here as the evaluation criteria including unit cell parameters (a, b, c, α, β, and γ), helium void fraction, pore volume, gravimetric surface area (GSA), largest cavity diameter (LCD), and pore-limiting diameter (PLD). Open-source Zeo++ code[23] was used to calculate pore volume, GSA, PLD, and LCD, and the radius of probe was set to be 0 Å. Helium void fraction was calculated by using RASPA simulation code with helium as probe atom.

3. RESULTS AND DISCUSSION

3.1 Performance of CoRE-MOFs in a natural gas purification setting

In our calculation, 2933 CoRE-MOFs with DDEC charges were extracted for analysis from CoRE-MOF database. GCMC simulations were employed to calculate the adsorption uptake of CO_2/CH_4 gas mixtures in these CoRE-MOF structures and adsorption selectivity of CO_2 over CH_4 and CO_2 working capacity were examined for PSA process, as shown in Figure 1.

Highly promising materials for PSA process always exhibit high selectivity as well as high CO_2 working capacity. In the study of screening zeolite structures for ethane/ethane mixtures, Kim[24] and his colleagues chose the product of selectivity and working capacity as a metric

that indicates the performance of a given structure. Following this idea, we used the similar method to identify the high-performance region. Two curves of reference performance were defined to identify the promising candidates. The product of selectivity and working capacity (SW) was set to be 100 and performed as one boundary of the high- and low-selectivity region. At the same time, ΔN_{CO_2}=1.3mol/kg was also chosen to separate high- and low-working capacity region.Finally, a high-performance region was identified (the red region in Figure 1) and 120 materials were exacted for further study. For these 120 CoRE-MOFs with good adsorption performance, we plotted the distribution histograms of their pore limiting diameters (PLD) and largest cavity diameters (LCD), as shown in Figure 2. From the distribution histograms, we could find that for most of the good performance CoRE-MOFs, their PLD and LCD are in the range of 2.5-6 Å and 3-7 Å respectively.

It is well known that pore channel structures and pore size of materials are vital for the adsorption separation process. Appropriate pore size could promote the adsorption of small gas molecules into the porous materials, while blocking the big gas molecules which try to enter into the pore channels. Thus in the work, we also plotted the graphs of CO_2/CH_4 selectivity versus PLD and LCD, as shown in Figure 3. There exists strong correlation between selectivity and PLD as well as LCD. The best range of LCD and LCD for the application of CO_2/CH_4 separation are 2.5-5 Å and 3-7 Å respectively.

3.2 The impact of desolvation on the MOF structures

In Sholl's previous work, he and his colleagues reported structures optimized using periodic density functional theory (DFT) for more than 800 experimentally synthesized metal-organic frameworks (MOFs)[25]. However, most of the good-performance MOFs which was found in our work could not be found in their optimized CoRE-MOF database. Thus we performed similar periodic DFT calculation to refine the selected 120 CoRE-MOFs with

good performance and 92 optimized structures were successfully obtained. After the structure optimization, many CoRE-MOF structures experienced various degrees of deformation, like the apparent shrink (Figure 4a) or expand (Figure 4b) of pores, and the structural changes of pore channels (Figure 4c). Among these materials, GUSNEN (ie. MIL-53, Figure 4b) whose pore channels expanded after structural optimization had been proved to be a flexible material and had strong breathing effect before and after desolvation[26]. Thus we removed it from our database and would not study it any more.

By comparing the structure changes among experimental structures (CCDC structures), CoRE-MOF structures and optimized structures upon solvent removal, we found that most of them exhibited obvious changes in the bond connections between activated metals and nearby organic components. By checking their original structures (CCDC structures), we found that there were always some solvent molecules binding with the metals and performing as a part of the structures. Once the bound solvent molecules were removed, the metals would be unsaturated, become open metal sites and want to build new bonds with the adjacent components to make the whole system saturated. The strong attraction of unbalanced open metal sites led to the rotation or the movement of organic group towards the unsaturated metals, resulting in the deformation of material structures or pore channels. Figure 5 exhibited two typical examples whose bond connections changed obviously. For the rest of unstable materials which no different bond connections were detected but still deformed a lot, we still found the movement of surrounding ligands towards the open metal sites (Figure 6).

In order to explore the impact of desolvation on the structural properties of MOFs, the changes in six parameters of unit cell and five geometrical properties were calculated and summarized in Figure 7. For more than half of the structures, the changes in unit cell lengths and angles were less than 12% and 7° respectively, and the percent difference in helium void fraction, surface area, pore volume, PLD and LCD were less than 40%, 20%, 30%, 25% and

20% respectively. From the box and whisker diagrams, we could also detect that even though half of the good performing CoRE-MOFs showed little changes in structural characteristics after DFT-optimization, there were still many CoRe-MOFs exhibited great differences in the structural and geometrical properties. The greatest changes in helium void fraction could even reach 100%.

The structures in CoRE-MOF database derived from Cambridge Structural Database, and all the materials have already been synthesized successfully by experiments. Thus there was no doubt that all the structures were stable before solvent removal. Based on this reality, relatively stable optimized-structures could be initially identified by comparing the differences between CoRE-MOF structures and their corresponding refined structures. If the structures did not change too much after structural optimization, we could say that solvent did not have great impact on the structures of the materials and it was less possible to collapse during the experimental fully activated process. Here, we set the percent changes in unit cell lengths and angles as 12% and 7°, and treated them as the critical values for the structure property changes of relatively stable materials. Then we set the boundary value of geometry property changes as 30% meaning that the changes in all 6 geometry characteristics mentioned above were less than 30% for relatively stable materials. Based on these screening criteria, about 50% of the potential materials were filtered out. And the remaining 50% optimized structures could be treated as relatively stable structures and extracted for further adsorption performance study.

3.3 Adsorption performance of relatively-stable optimized-structures.

In the previous research of Nazarian and his colleagues, they made a comparison of DDEC charges predicted for each atom type of 879 MOF structures before and after structure optimization and found that the changes in DDEC point charges associated with relaxation

were not obvious and could be negligible[25]. Thus, in this work, the same DDEC charges in CoRE-MOFs were applied to their optimized structures to test the adsorption performance of the relatively-stable refined-structures, as shown in Figure 8.

From Figure 8, we could find that the adsorption performance of most selected stable refined-structures decreased a lot and only 12 optimized structures were still in the high-performance region. This phenomenon implied that the gas adsorption was extremely sensitive to the slight changes of structures. The adsorption results of the top-performing refined structures was listed in Table 1.

We compared the differences in CO_2 working capacity and selectivity of CO_2 over CH_4 between the selected 50 CoRE-MOF structures and their corresponding DFT-optimized structures, as shown in Figure 9. The results showed that for most of the selected CoRE-MOFs, the adsorption selectivity decreased a lot after structural optimization. However, for the CO_2 working capacity, structural optimization played different roles for different materials.About 21% of the selected structures remained unchanged in the CO_2 working capacity and 19% showed enhancement in CO_2 working capacity upon refinement. The remaining 60% exhibited reduction in the CO_2 working capacity.

We also plotted the changes in mixture uptake of CO_2 and CH_4 between the structure found in the CoRE-MOF database and DFT-optimized structure at 1bar and 10bar, as shown in Figure10. It could be easily found that for most of the relatively-stable materials, the mixture uptake of CO_2 decreased and that of methane increased.

For the selected relatively-stable materials, as their pore volume and surface area did not significantly change before and after structural optimization, it is reasonable to ignore the impact of pore volume and surface area on the adsorption separation performance. Thus, in order to explore the reason of this phenomenon, we examined the configuration details of

unsaturated metals and their coordinating ligands in pre- and post-optimized CoRE-MOFs. Surprisingly, we found that for most materials, the unsaturated metals become saturated after DFT-optimization. In other words, for the structures in CoRE-MOF database, the structures were treated rigid in the process of solvent removal and the open metal sites always exposed to the pore channels and were accessable for incoming guest molecules. But in fact, the removal of solvent would lead to the rearrangment or aggregation of linkers towards the unsaturated sites, restricting access to guest molecules. Figure 11 showed one typical example of the rearrangement of organic linkers after DFT-optimization. For this MOF, no obvious changes happened in the MOF structure but the CO_2 adsorption performance decreased by 40%. From Figure 11, it is easy to detect the aggregation of organic linker towards the metals and the less expossure of metals to the accessible pore channels. Furthermore, it has been shown that open metal sites could greatly improve the performance of selective separation because of the significant enhancement in the adsorption of strongly binding gas like CO_2[4-8]. In this work, optimal materials have small pore channels which were suitable for CO_2, and a slight movement of unsaturated metals or organic linkers obstruct the active binding sites of CO_2 molecules. This weakened the interaction between unsaturated metal sites and CO_2, resulting in the sharp reduction of CO_2 uptake and the selectivity of CO_2 over CH_4. Moreover, as the CO_2 working capacity was the CO_2 loading difference between high- and low- pressure. Thus, the magnitude of reduction in CO_2 loading at high- and low-pressure had great impact on the CO_2 working capacity and led to the enhancement or reduction of CO_2 working capacity.

4. CONCLUSIONS

In this work, a multi-level screening process was proposed to deeply study the CoRE-MOF database for the application of natural gas purification. Instead of screening CoRE-MOF

database only by calculating adsorption performance of CoRE-MOFs, we also take the stability of the materials upon desolvation into account and set it as a critical criterion for the selection of optimal MOFs with open-metal sites. In our screening process, we found that many good performing CoRE-MOFs undergo different levels of deformation even collapse after desolvation. The strong attraction of unsaturated metal sites with the surrounding ligands resulted in the collapse and deformation of the pore channels. For the selected potential materials which did not change too much after structural optimization, we found that most of their optimized-strucutures could not reach that good performance as that in CoRE-MOF structures, especially for the adsorption selectivity of CO_2 over CH_4. The primary reason of this phenomenon is that the open-metal sites become not that accessible for the guest molecules and the increase of the resistance between the unsaturated metal sites and strongly binding gas CO_2 which eventually resulted in the great reduction of CO_2 uptake. This work could be served as a guidance for the experimental synthesis and also a reminder for the other studies of CoRE-MOF database.

Notes

The authors declare no competing financial interest.

ACKNOWLEDGMENTS

The financial support received from the National Natural Science Foundation of China (21908116) are gratefully acknowledged.

REFERENCES

1. Yang RT. *Gas Separation by Adsorption Processes*. Butterworths, Boston, MA, 1987.
2. Farha OK, Bae YS, Hauser BG, Spokoyny AM, Snurr RQ, Mirkin CA, Hupp JT. Chemical

reduction of a diimide based porous polymer for selective uptake of carbon dioxide versus methane. *Chem. Commun.* 2010, 46, 1056-1058.

3. Wilmer CE, Farha OK, Bae YS, Hupp JT, Snurr RQ. Structure-property relationships of porous materials for carbon dioxide separation and capture. *Energy Environ. Sci.* 2012, 5, 9849-9856.
4. Chen B, Yang Y, Zapata F, Lin G, Qian G, Lobkovsky EB. Luminescent open metal sites within a metal-organic framework for sensing small molecules. *Adv. Mater.* 2007, 19, 1693-1696.
5. Queen WL, Hudson MR, Bloch ED, Mason JA, Gonzalez MI, Lee JS, Gygi D, Howe JD, Lee K, Darwish TA, James M, Peterson VK, Teat SJ, Smit B, Neaton JB, Long JR, Brown CM. Comprehensive study of carbon dioxide adsorption in the metal-organic frameworks M2 (Dobdc) (M = Mg, Mn, Fe, Co, Ni, Cu, Zn). *Chem. Sci.* 2014, 5, 4569-4581.
6. Kong X, Scott E, Ding W, Mason JA, Long JR, Reimer JA. CO_2 dynamics in a metal-organic framework with open metal sites. *J. Am. Chem. Soc.* 2012, 134, 14341-14344.
7. Lin LC, Kim J, Kong X, Scott E, McDonald TM, Long JR, Reimer JA, Smit B. Understanding CO_2 dynamics in metal- organic frameworks with open metal sites. *Angew. Chem.* 2013, 125, 4506-4509.
8. Poloni R, Lee K, Berger RF, Smit B, Neaton JB. Understanding trends in CO_2 adsorption in metal-organic frameworks with open-metal sites. *J. Phys. Chem. Lett.* 2014, 5, 861-865.
9. Lee K, Howe JD, Lin LC, Smit B, Neaton JB. Small- molecule adsorption in open-site metal-organic frameworks: a systematic density functional theory study for rational design. *Chem. Mater.* 2015, 27, 668-678.
10. Chung YG, Camp J, Haranczyk M, Sikora BJ, Bury W, Krungleviciute V, Yildirim T, Farha OK, Sholl DS, Snurr RQ. Computation-ready, experimental metal-organic frameworks: a tool to enable high-throughput screening of nanoporous crystals. *Chem.*

Mater. 2014, 26, 6185-6192.

11. Qiao ZW, Zhang K, Jiang JW. In silico screening of 4764 computation-ready, experimental metal-organic frameworks for CO_2 separation. *J. Mater. Chem. A*. 2016, 4, 2105-2114.
12. Li S, Chung G, Snurr R. High-throughput screening of metal-organic frameworks for CO_2 capture in the presence of water. *Langmuir.* 2016, 32, 10368-10376.
13. Simon CM, Kim J, Gomez-Gualdron DA, Camp JS, Chung YG, Martin RL, Mercado R, Deem MW, Gunter D, Haranczyk M, Sholl DS, Snurr RQ, Smit B. The materials genome in action: identifying the performance limits for methane storage. *Energy Environ. Sci.* 2015, 8, 1190-1199.
14. Potoff JJ, Siepmann JI. Vapor-liquid equilibria of mixtures containing alkanes, carbon dioxide, and nitrogen. *AIChE J*. 2001, 47, 1676-1682.
15. Martin MG, Siepmann JI. Transferable potentials for phase equilibria. 1. united-atom description of n-alkanes. *J. Phys. Chem. B*. 1998, 102, 2569-2577.
16. Mayo SL, Olafson BD, Goddard III WA. DREIDING: a generic force field for molecular simulations. *J. Phys. Chem.* 1990, 94, 8897-8909.
17. Rappe AK, Casewit CJ, Colwell KS, Goddard III WA, Skiff WM. UFF, a full periodic table force field for molecular mechanics and molecular dynamics simulations. *J. Am. Chem. Soc.* 1992, 114, 10024-10035.
18. Nazarian D, Camp JS, Sholl DS. A comprehensive set of high-quality point charges for simulations of metal-organic frameworks. *Chem. Mater*. 2016, 28, 785-793.
19. Ewald PP. Die berechnung optischer und elektrostatischer gitterpotentiale. *Ann. Phys.* 1921, 369, 253-287.
20. Braun E, Zurhelle AF, Thijssen W, Schnell SK, Lin LC, Kim J, Thompsonf JA, Smit B. High-throughput computational screening of nanoporous adsorbents for CO_2 capture from natural gas. *Mol. Syst. Des. Eng.* 2016, 1, 175-188.

21. Giannozzi P, Baroni S, Bonini N, Calandra M, Car R, Cavazzoni C, Ceresoli D, Chiarotti GL, Cococcioni M, Dabo I, Dal Corso A, de Gironcoli S, Fabris S, Fratesi G, Gebauer R, Gerstmann U, Gougoussis C, Kokalj A, Lazzeri M, Martin-Samos L, Marzari N, Mauri F, Mazzarello R, Paolini S, Pasquarello A, Paulatto L, Sbraccia C, Scandolo S, Sclauzero G, Seitsonen AP, Smogunov A, Umari P, Wentzcovitch RM. QUANTUM ESPRESSO: A modular and open-source software project for quantum simulations of materials. *J. Phys.: Condens. Matter.* 2009, 21, 395502.

22. Perdew JP, Ruzsinszky A, Csonka GI, Vydrov OA, Scuseria GE, Constantin LA, Zhou X, Burke K. Restoring the density-gradient expansion for exchange in solids and surfaces. *Phys. Rev. Lett.* 2008, 100, 136406.

23. Willems TF, Rycroft C, Kazi M, Meza JC, Haranczyk M. Algorithms and tools for high-throughput geometry-based analysis of crystalline porous materials. *Microporous Mesoporous Mater.* 2012, 149, 134-141.

24. Kim J, Lin LC, Martin RL, Swisher JA, Haranczyk M, Smit B. Large-scale computational screening of zeolites for ethane/ethene separation. *Langmuir.* 2012, 28, 11914-11919.

25. Nazarian D, Camp JS, Chung YC, Snurr RQ, Sholl DS. Large-scale refinement of metal-organic framework structures using density functional theory. *Chem. Mater.* 2017, 29, 2521-252.

26. Serre C, Millange F, Thouvenot C, Noguès M, Marsolier G, Louër D, Férey G. Very large breathing effect in the first nanoporous chromium(III)-based solids: MIL-53 or $Cr^{III}(OH)\cdot\{O_2C\text{-}C_6H_4\text{-}CO_2\}\cdot\{HO_2C\text{-}C_6H_4\text{-}CO_2H\}_x\cdot H_2O_y$. *J. Am. Chem. Soc.* 2002, 124, 13519-13526.

Table 1. The adsorption properties of the top-performing refined structures

Name	ΔN_{CO_2} (mol/kg)	S_{ads} (CO_2/CH_4) (10bar)
GIQXIO	1.490762073	153.1421241
GIQXUA	1.962694394	110.9543548
GIQYAH	1.914343565	101.9244733
GIQYEL	1.634344571	84.40233143
GIQYIP	1.52018303	145.7173852
KAPHOZ	2.526982894	62.28929092
LOBHAM	4.130477871	24.36178594
OXAMIK	1.818739018	78.65314392
QAVDEW	1.728042996	72.09376472
UHISOU	2.142083479	63.49105066
WIYZOU	2.375503731	75.74029216
XANMIJ	3.382545222	42.62258436

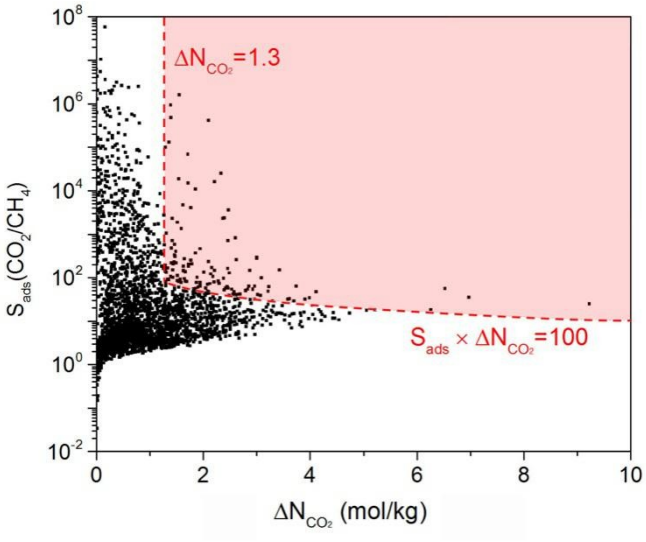

Figure 1. Adsorption selectivity (S_{ads}) vs CO_2 working capacity (ΔN_{CO_2}) of CoRE-MOFs for the separation of CO_2/CH_4 gas mixture.

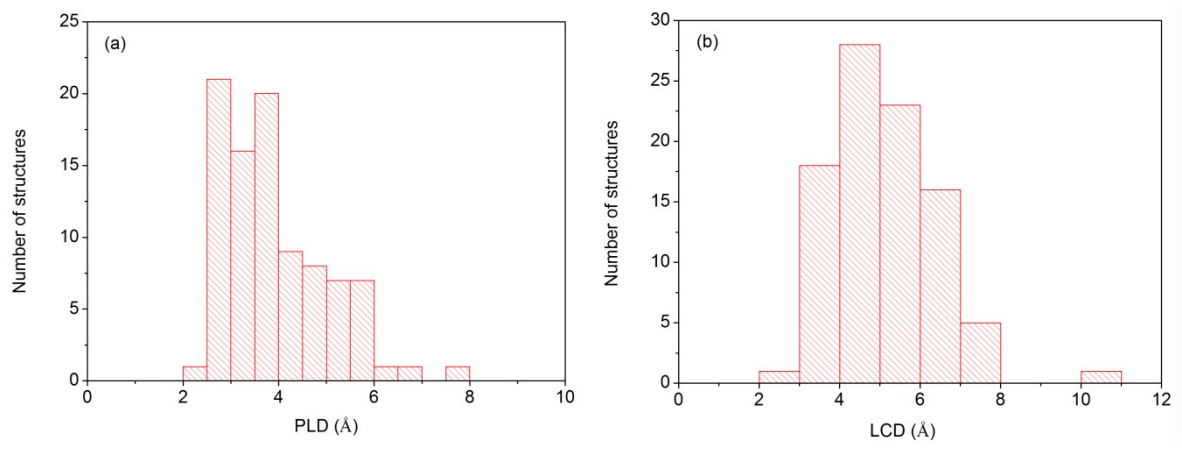

Figure 2. Histograms of (a) PLD and (b) LCD for 120 potential CoRE-MOFs.

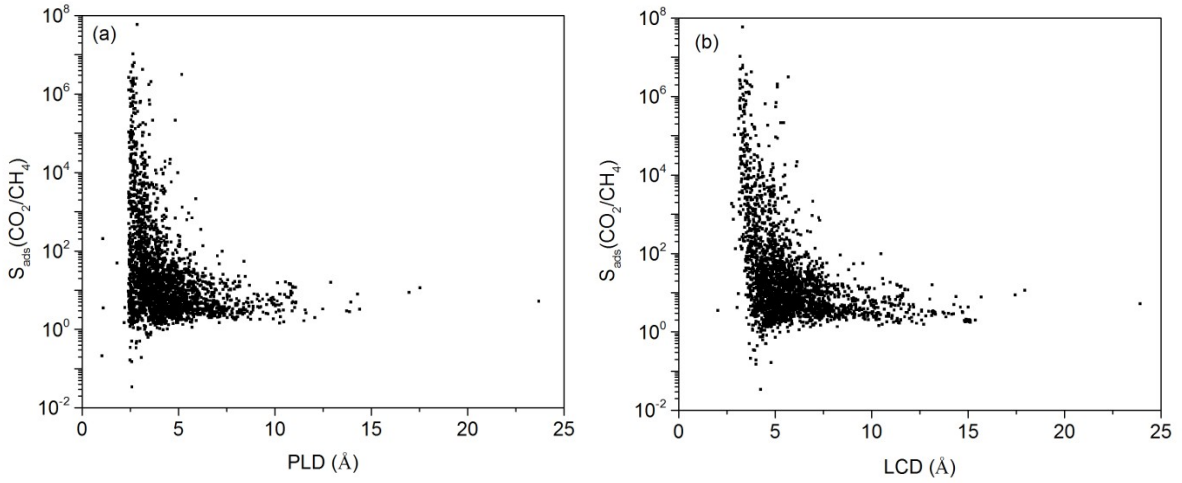

Figure 3. Relationships between adsorption selectivity (S_{ads}) and (a) PLD as well as (b) LCD.

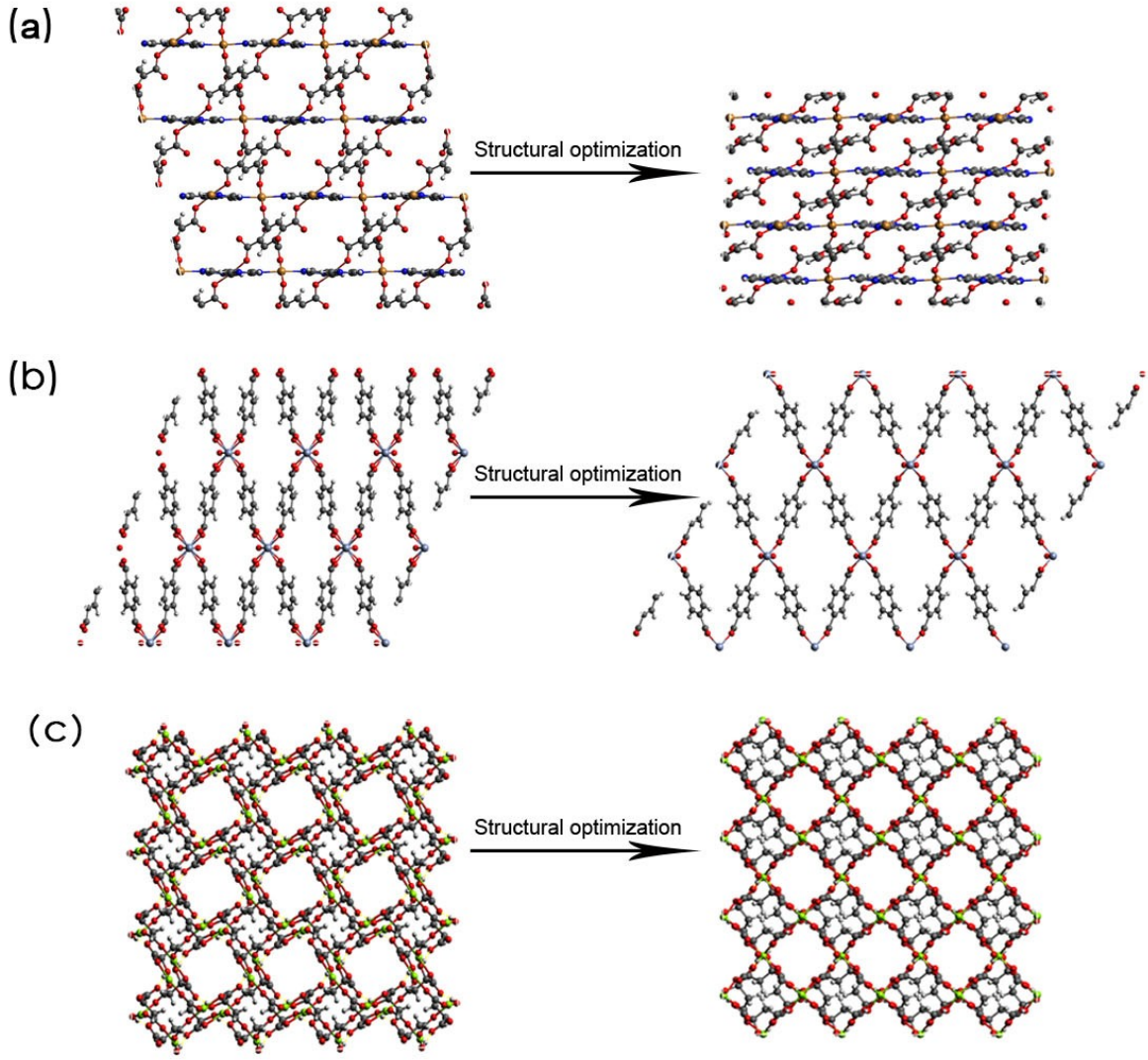

Figure 4. Some typical MOFs which exhibited obvious deformation after structural optimization. (left) The structures which were found in CoRE-MOF database and (right) their corresponding optimized-structures: (a) XADFAL, (b) GUSNEN and (c) DORFOG.

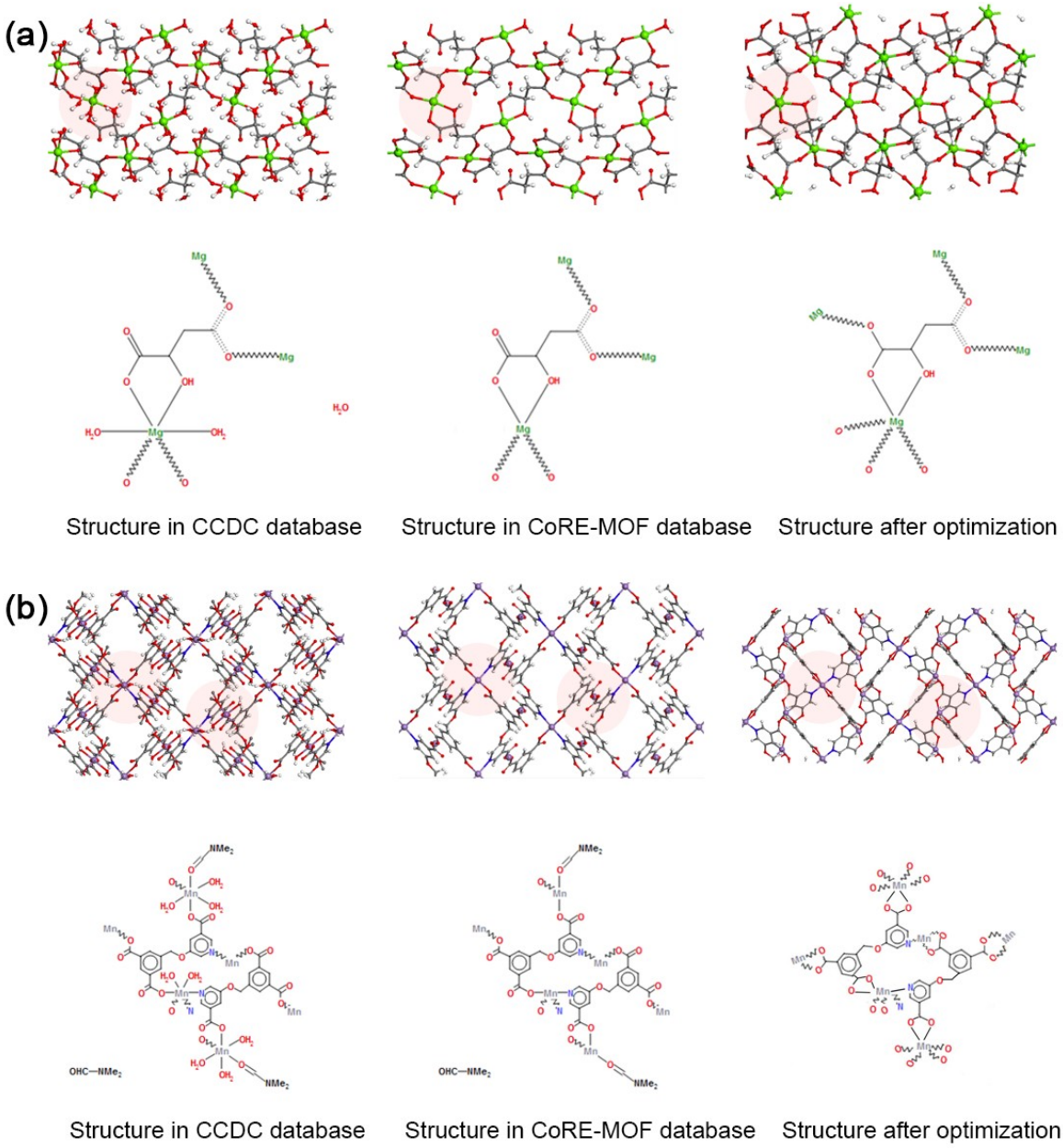

Figure 5. Two typical MOFs which exhibited obvious changes in bond connections after solvent removal: (a) DORFOG and (b) BEXSAA.

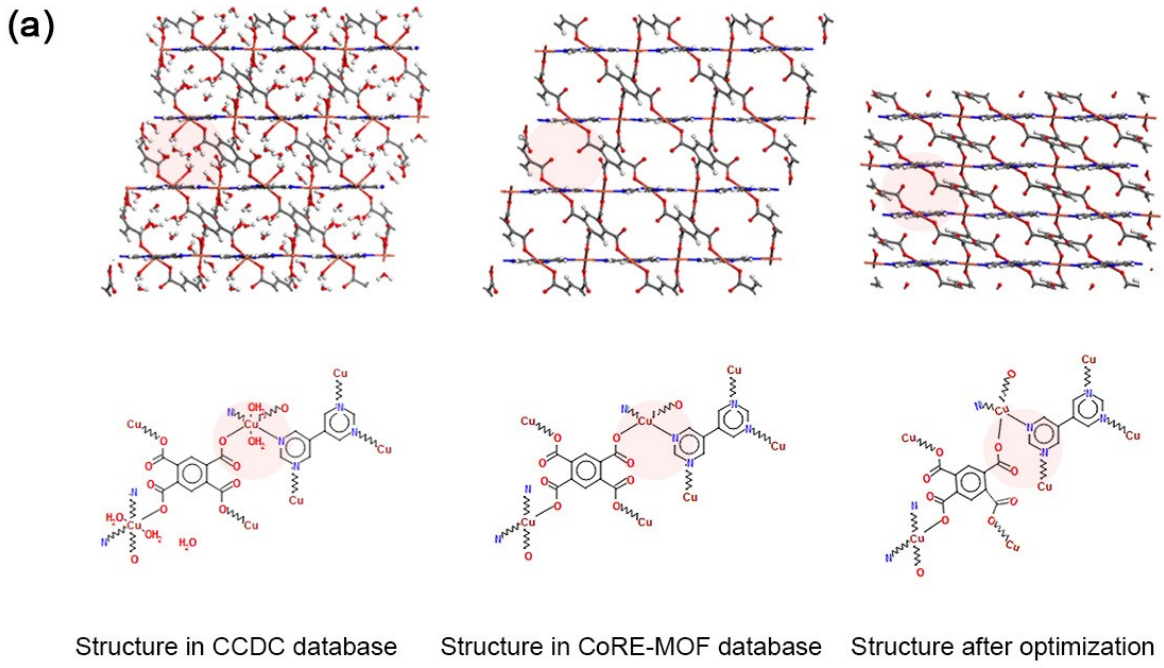

Figure 6. One typical MOF which deformed a lot but no obvious changes in bond connections after solvent removal: (a) XADFAL.

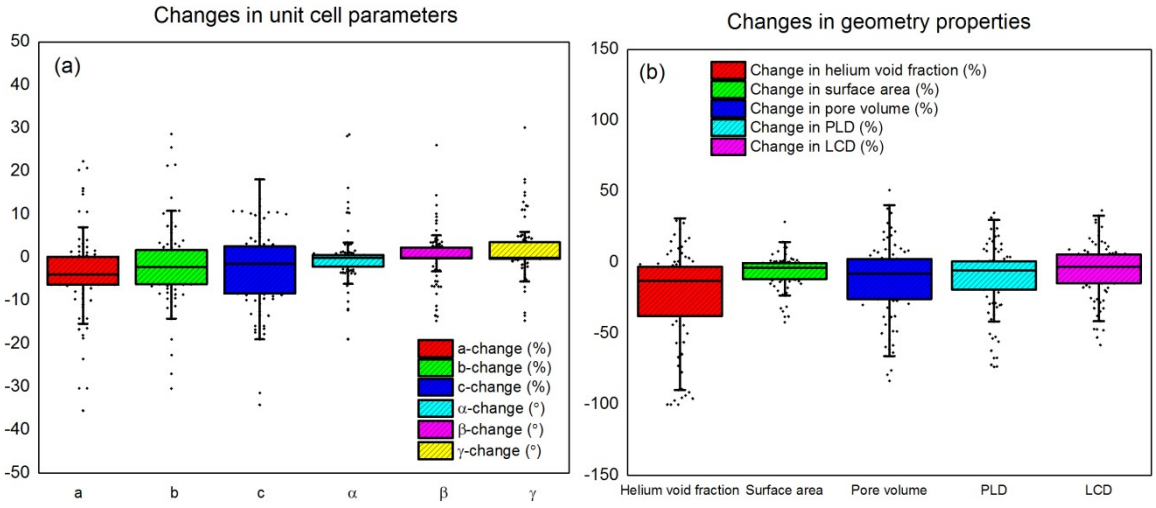

Figure 7. Box and whisker diagrams for changes in (a) unit cell parameters and (b) geometry properties.

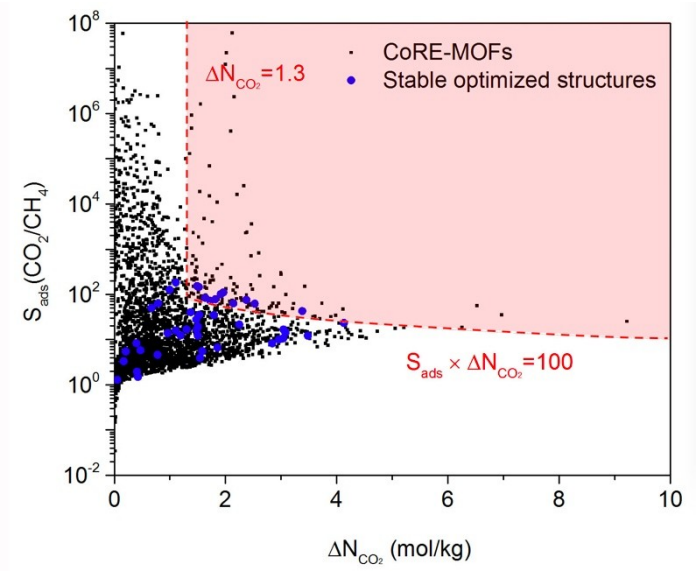

Figure 8. Adsorption selectivity (S_{ads}) vs CO_2 working capacity (ΔN_{CO_2}) of 2933 CoRE-MOFs and 50 stable optimized-structures for the separation of CO_2/CH_4 gas mixture.

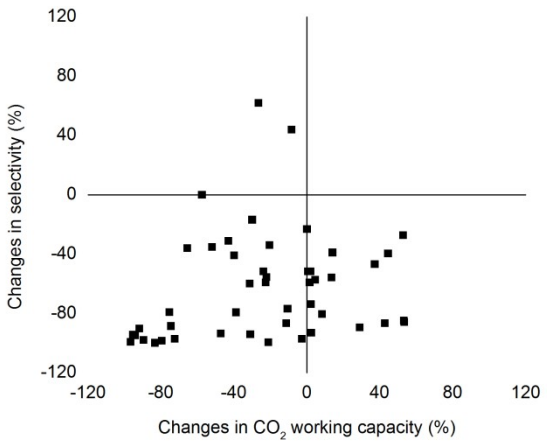

Figure 9. Percent difference in CO_2 working capacity and selectivity of CO_2 over CH_4 (10 bar) between the structure found in the CoRE-MOF database and DFT-optimized structure.

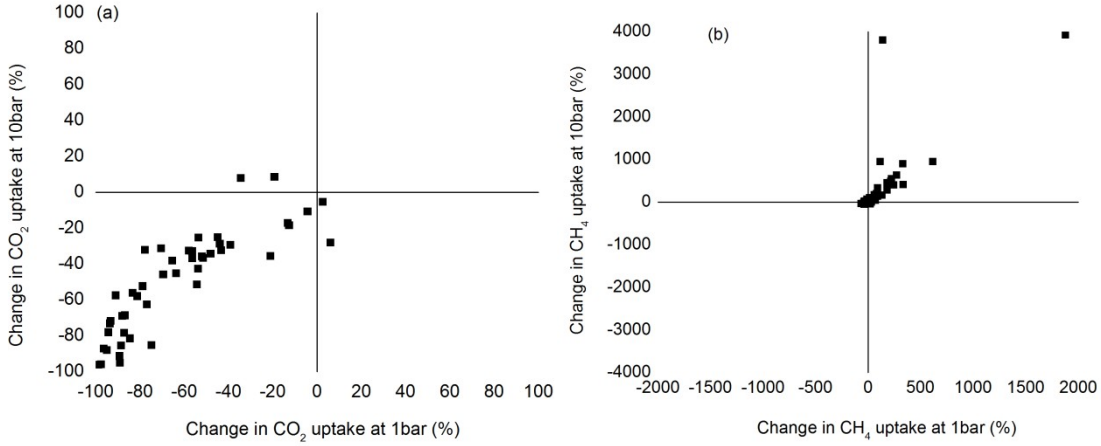

Figure 10. Percent difference in mixture uptake of (a) CO_2 and (b) CH_4 between the structure found in the CoRE-MOF database and DFT-optimized structure.

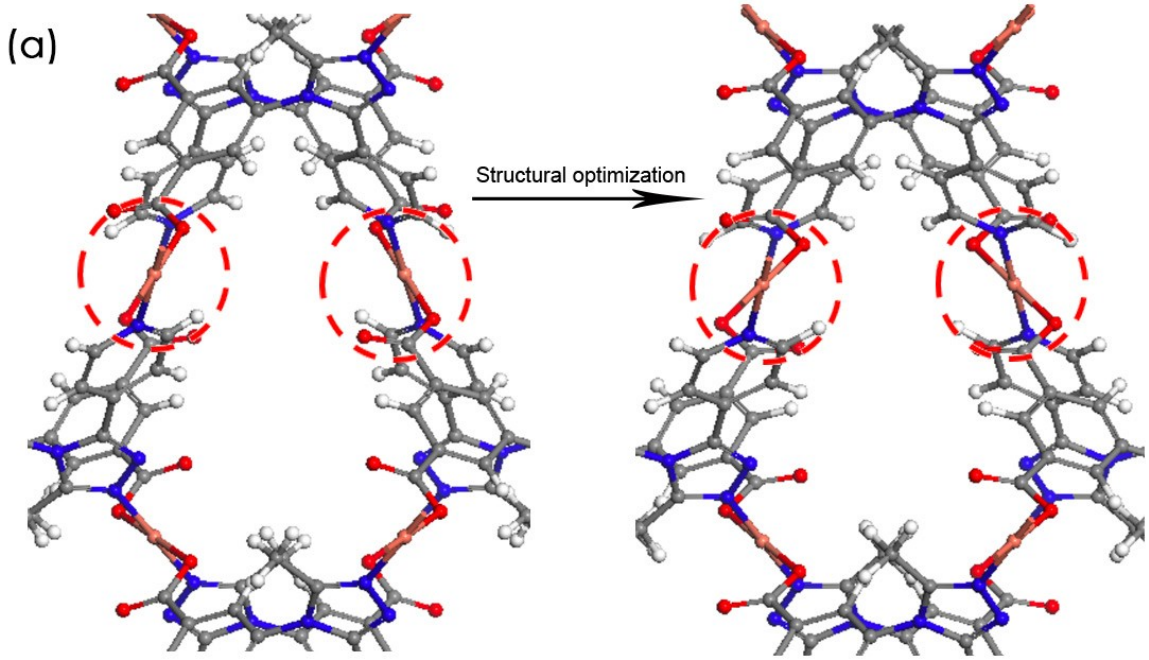

Figure 11. One typical example of the rearrangement of organic linkers after DFT-optimization: (a) DABWUA.